

Generation of a flat-top laser beam for gravitational-wave detectors by means of a non-spherical Fabry-Perot resonator

Marco G. Tarallo^{1,2}, John Miller³, J. Agresti^{1,2}, E. D'Ambrosio², R. DeSalvo²,
D. Forest⁴, B. Lagrange⁴, J. M. Mackowsky⁴, C. Michel⁴, J. L. Montorio⁴,
N. Morgado⁴, L. Pinard⁴, A. Remilleux⁴, B. Simoni^{1,2}, P. Willems²

¹*Dipartimento di Fisica presso Università di Pisa, Largo Pontecorvo 3, 56100 Pisa, Italy*

²*LIGO Laboratory, 1200 E. California Blvd., Pasadena CA, United States*

³*Physics and Astronomy, University of Glasgow, Glasgow, G12 8QQ, UK*

⁴*Laboratoire des Matériaux Avancés, 22 Bd. Niels Bohr, Villeurbanne, France*

marco.tarallo@pi.infn.it

We have tested a new kind of Fabry-Perot long-baseline optical resonator proposed to reduce the thermal noise sensitivity of gravitational wave interferometric detectors—the *mesa beam* cavity, whose flat top beam shape is achieved by means of an aspherical end mirror. We present the fundamental mode intensity pattern for this cavity and its distortion due to surface imperfections and tilt misalignments, and contrast the higher order mode patterns to the Gauss-Laguerre modes of a spherical mirror cavity. We discuss the effects of mirror tilts on cavity alignment and locking and present measurements of the mesa beam tilt sensitivity.

© 2007 Optical Society of America

OCIS codes: 140.4780, 120.2230, 230.0040

1. Introduction

Most gravitational wave interferometric detectors (GWIDs) measure the variation in phase between light beams resonating in two perpendicular cavities caused by the passage of a gravitational wave. Any physical displacement of the reflective surfaces of the cavity mirrors also creates phase variations and thus contributes noise to the measurement. In particular, random displacements of the test masses' reflective surfaces due to thermodynamical

fluctuations is a major source of fundamental noise in the frequency range of maximum sensitivity.¹

Gaussian laser beams are typically used to measure the position of the mirrors in these new detectors. It is possible to significantly reduce the measured test mass thermal noise using modified optics that reshape the beam from the conventional gaussian intensity profile into a flat-top beam profile. Thorne and others proposed and theoretically studied^{2,3,4} the possibility of using a particular class of aspherical mirrors, the so-called ‘‘Mexican-hat’’ (MH) mirrors, in a Fabry-Perot cavity in order to generate a wider, flat top laser beam, the *mesa beam*. Such a beam is predicted to significantly reduce all sources of test mass thermal noise by better averaging over surface fluctuations.^{2,3,4,6,7,8}

The mesa electromagnetic field is a superposition of minimal-Gaussian fields whose axes are parallel to the cavity axis and lie within a cylinder of radius r_{mesa} centered on the cavity axis. The (non-normalized) field distribution over the mirror surface is

$$\begin{aligned} U(r) &= \int_{r' \leq r_{mesa}} \exp\left(-\frac{(r - \vec{r}')^2(1 - i)}{2w_0^2}\right) d^2\vec{r}' \\ &= 2\pi \int_0^{r_{mesa}} \exp\left(-\frac{(r^2 + r'^2)(1 - i)}{2w_0^2}\right) I_0\left(\frac{rr'(1 - i)}{w_0^2}\right) r' dr' \end{aligned} \quad (1)$$

where I_0 is the modified Bessel function of zeroth order and $w_0 = \sqrt{L/k}$ is the waist of the minimal-Gaussian (where L is the length of the cavity and k is the wavenumber). For a cavity to have the mesa beam as an eigenmode, the surfaces of the mirrors must coincide with one of the mesa field’s surfaces of constant phase (this is strictly true only for mirrors of infinite radius, but is quite a good approximation for finite mirrors if the diffraction losses are small). The resulting height distribution as a function of the radial distance r is given by⁴

$$h_{MH} = \frac{Arg[U(r)] - Arg[U(0)]}{k} \quad (2)$$

To evaluate the feasibility of this concept, we have designed and built a mesa beam cavity.⁹ The aim of this experiment is to explore the main properties of a single optical cavity before any eventual use in a second generation gravitational-wave interferometer. In particular, we are interested in studying the experimental mesa field achievable with realistically imperfect mirrors and how its behavior differs from that of a gaussian field with respect to perturbations such as cavity misalignments.

2. The experiment

We designed the experiment to produce a resonant beam that could be directly scaled for application in an Advanced LIGO Fabry-Perot arm cavity (arm length $L_{AdLIGO} = 4\text{km}$).

The relation between the Fabry-Perot cavity length and the beam radius is^{2,4}

$$r_{mesa} = 4\sqrt{\frac{2\pi L}{\lambda}}. \quad (3)$$

Hence, to maintain the correct proportions, the length $L_{prototype}$ of the prototype must be

$$L_{prototype} = \left(\frac{r_{mesa}^{prototype}}{r_{mesa}^{AdLIGO}}\right)^2 L_{AdLIGO}. \quad (4)$$

Our MH mirror production technique sets the main constraint to the prototype geometry. It consists of a three step silica deposition process over a micro-polished flat substrate, which can achieve up to 2 nm precision.⁵ However, the maximum slope measurable by our metrological apparatus is 500 nm/mm. This sets the radius of the smallest feasible mesa beam made using our technique to about 6 mm. For a fixed diffraction loss, the MH mirror profile height does not depend on the cavity length. This means that the MH mirror shape is simpler to realize on large mirror substrates (as in the GWID case) than on our smaller mirrors. Other groups have demonstrated mesa beam cavities using deformable mirrors,^{10,11} but such mirrors are not obviously usable in low-noise gravitational wave interferometry.

Our smallest practical mirror size sets our cavity length to ~ 16 meters. We further reduced the physical length of the structure to ~ 8 m by building a half-symmetric cavity (a single MH mirror paired with a flat mirror at what would be the midpoint of a full length cavity) and then to ~ 4 m by folding. In this way it was possible to build a rigid suspended cavity.

Fig. 2 shows the suspended cavity. Three Invar rods fix the cavity length to $L_{prototype} = 2 \times 3.657 \text{ m} = 7.32 \text{ m}$, with a folding mirror at one end of the structure and the input and end mirrors on the other end. Five triangular spacers maintain structural rigidity, with the outer two spacers bolted at the ends of the structure and containing the mirror mounts. The cavity is suspended by two pairs of maraging steel wires from GAS (Geometric-Anti-Spring)¹² blades, providing both horizontal and vertical isolation. The whole is suspended in an aluminum chamber for thermal stability and protection from air currents; this chamber is not evacuated.

The test MH mirror [Fig.3] was designed using the waist size of the minimal gaussian with $L = 2L_{prototype}$ as a reference length, so that the resulting mesa beam had a radius $r_{mesa} = 6.30 \text{ mm}$. We required that our test mirror have similar diffraction loss around its aperture as an Advanced LIGO test mass; in order to have 1 ppm diffraction loss the mirror radius was set to $R = 13 \text{ mm}$.

Due to the technical difficulties of the MH figure deposition on the flat substrate, the MH mirror had non-negligible figure error [see Fig.3(b)], mostly in the central bump where the height is just 27 nm. In particular, the figure error reaches a maximum of 5 nm at the edge

of the central bump. Before performing our experiment, we modeled our MH mirror profile using a Mathematica-based FFT routine that simulates beam propagation inside our cavity in the paraxial approximation regime. As was theoretically expected,⁴ the effect of such a surface figure error is comparable to a mirror tilt of $0.9 \mu\text{rad}$, which can be applied to the actual mirror to recover a flat top beam profile. These FFT results are discussed in more detail in section 4a.

The losses of our MH mirror were almost entirely due to its transmission, which averaged around 1000 ppm. The transmission was inhomogeneous, increasing slightly in the center, but this had no significant effect on the cavity performance.

The other two cavity mirrors were commercially available flats, 2 inches in diameter and 0.375 inches thick. The folding mirror had a high reflectivity ($R=0.999$) dielectric coating, while a power reflectivity of 0.95 was chosen for the input mirror. These values give a theoretical cavity finesse of about 110. Two aluminum spacer rings were fixed to the two surfaces of the flat mirrors using Vac-seal epoxy to minimize flexure due to point contacts in the mirror mounts.

Our 7.32 m cavity has a free spectral range $\Delta\nu_{FSR} = 20.49$ MHz. The width of the spectral lines without taking into account losses is expected to be $\Delta\nu_{FWHM} = 0.184$ MHz. We numerically calculated the expected transverse mode frequency distribution by solving the eigenequation for a two-mirror optical resonator. Unlike the case for a spherical mirror resonator, the transverse modes inside a mesa cavity do not exhibit a symmetric spacing. Nevertheless, the resonant frequencies still increase with mode order, with a frequency separation of the order 0.5 MHz, as shown in Table 1. The finesse is high enough that there is sufficient spacing between adjacent modes to prevent mixing and allow lock acquisition onto an individual mode.

Figure 1 shows the optical layout. We use a Mephisto 800ME Nd:YAG laser as input to the cavity. The beam is nearly collimated at the input mirror surface, with a spot size of about 6.06cm and a wavefront radius of curvature greater than 28 m. With this beam the expected input power coupling efficiency is 99.6 % of optimal coupling.⁴

We measured the transverse profile of the cavity beam leaking through the folding mirror using a Coherent LaserCam IIID CCD beam profiler. By scanning a HeNe laser beam across the CCD array, we measured the gain uniformity over the camera array to be about 1.5%, with a maximum pixel-to-pixel relative error of 5.9%. The leakage field through the MH end mirror was used for a simple dither-lock servo in which the cavity length was modulated using PZTs on the folding mirror. Additional details of the experimental setup are available in the thesis of Tarallo.¹³

3. Alignment of a mesa beam cavity

The greatest experimental difficulty was found in obtaining a sufficiently precise alignment to achieve a flat top power distribution in the cavity. In a cavity made with spherical mirrors, a tilted mirror presents the same spherical profile to the opposite mirror, but shifted sideways, and the cavity simply resonates the same transverse mode spectrum centered upon a shifted optical axis. In contrast, the MH mirror has a non-spherical shape, and any misalignment destroys the cylindrical symmetry of the cavity. In such a situation the resonant beam senses a mirror with a suboptimal profile and the cavity mode will thus have a radically different intensity distribution and phase front.

When our cavity was in such a misaligned state, higher order and distorted modes were found easily (see Fig.4). However, only asymmetric fundamental modes could resonate. An example of such a mode is plotted in Fig.5(a). Any attempt to reduce the asymmetry resulted in an extremely tilt-sensitive power distribution until the mode settled in a similar asymmetric shape with a different orientation. An example of this fundamental mode is shown in Fig.5(b).

The extreme sensitivity to misalignment proved to be caused by our nominally flat folding and input mirrors, which had surface deviations of order 60-100 nm from flatness before we epoxied the aluminum spacers to them.

4. Results

4.A. The fundamental mode

Having reduced the flat mirrors' flexure, it was possible to lock the cavity to a stable fundamental mode with nearly uniform distribution. In fact, taking into account the residual warping of the flat mirrors and MH mirror imperfections, this mesa beam is consistent with the best achievable using our current prototype MH mirror [see Fig. 6].

Figure 7 shows four beam profiles. Two are experimental data, smoothed with a 0.1 mm (5 pixels) gaussian kernel to clean them of digitization noise and dust diffraction rings. The other two are profiles simulated using our FFT code. The simulated profiles represent the leakage field at the output bench (~ 5 meters from the input mirror) achieved applying the ideal corrective tilt at the MH mirror.

The qualitative agreement between measurement and simulation indicates that the deviations from the theoretical profile are likely dominated by mirror defects, rather than misalignments. In particular, the FFT simulations show that the imperfect profile of the MH mirror creates a jagged profile at the nominally flat top of the mesa profile.

The mesa beam width (defined as four times the second moment of the intensity profile) was measured to be $w_{exp} = 6.8 \pm 1.1$ mm, which is consistent with the $w_{theo} = 6.68$ mm

predicted by the FFT code for this cavity at the plane of the beam scanning CCD.

Another systematic error in our experiment is the surface deviations of the two flat cavity mirrors, particularly the astigmatism of the input mirror. Using a Fizeau interferometer, we found these mirrors to be astigmatic, this astigmatism causing both a jagged diffraction pattern on the top of the flat top mesa beam profile and an ellipticity of the mesa beam.¹⁴ These values cause an increase of the beam width along the y axis with respect to the x axis of 0.4% for the best-fit spherical end mirror to the MH test mirror. Experimentally this asymmetry is 7.7% in our mesa beam cavity. Although the MH ellipticity is more than ten times larger, the beam deforms in the position and direction predicted by this approximation. The mirror warping also reduces the cavity finesse. By comparing the resonance linewidth to the cavity free spectral range, we measure the finesse to be 65 ± 3.6 instead of the expected 110.

The FFT simulated cavity fundamental mode (Fig. 7) shows some deviations from the theoretical mesa beam intensity pattern and sets the maximum limit to the best achievable mesa beam. The ripples in the central area set a limitation of about 7.5% peak-to-valley amplitude on the flatness of the power distribution on the top of the beam. However the steep fall on the edges and the width of the beam should be, and are, very close to the ideal perfect mirror case. Analyzing the profile in Fig. 7, the normalized absolute power in the simulated profile not fitted by the mesa TEM₀₀ is 3.4%. By comparison, the normalized absolute power in the experimental profile not fitted by the mesa TEM₀₀ is 3.8%, after the normalization of the power on the CCD, with a peak to valley deviation from the flat profile of about 9.4%. These numbers suggest that the resulting mesa beam is very close to the experimental limit due to the imperfect MH test mirror.

4.B. High order modes and spectral distribution

In Figure 8 we show some higher-order transverse mesa beam modes. These modes are superficially quite similar to the Laguerre-gaussian modes for a spherical mirror Fabry-Perot cavity. However, in the precise power distribution there are differences as shown in Figure 9. The experimental data is in good agreement with the expected mesa TEM₁₀ profile. As for the fundamental mode, there is some asymmetry due to the mirror imperfections.

5. Tilt sensitivity

Since the mesa beams are intended for use in actual interferometers it is important to study their ease of control. Some theoretical and experimental investigations have been carried out in this area.^{2,3,4,10} The alignment tolerances for a mesa beam arm cavity are expected to be ~ 3 times more stringent than those of the gaussian arm cavity in an advanced gravitational wave detector.

In our 7.3 m cavity (just as in a long baseline GWID), extremely small tilts create significant modification of the mesa beam profile. Nonlinearities and uncertainties in the mirror actuators obliged us to measure the mirror tilt directly, rather than infer it from the applied PZT voltages. Fig. 10 shows our setup. We reflected a HeNe laser optical lever beam off the MH mirror to a quadrant photodiode. The MH mirror tilt was then dithered using the alignment PZTs, and the quadrant PD difference signal sent to a lock-in detector. This made the tilt measurement insensitive to low-frequency jitter in the HeNe laser beam pointing. The cavity beam profile was captured by the beam scanner CCD at the maximum mirror tilt by triggering the CCD when an optical chopper wheel synchronized to the mirror tilt exposed the CCD to the cavity beam. The tilt precision of the optical lever is estimated to be $0.05 \mu\text{rad}$.

Figure 11 shows the good agreement between our recorded profiles (thin lines) and FFT simulated data (thick lines). Note that these FFT simulated profiles were constructed using a two-mirror cavity (as opposed to the real three-mirror cavity).

6. Conclusions

The results reported here are the first of a mesa beam cavity employing mirrors constructed in a manner applicable to sensitive gravitational-wave interferometers. We observe good agreement between theoretical and experimental results for the fundamental and higher order transverse modes. In particular, we achieved the flat-topped, steep-sided optical power distribution necessary to reduce thermal noise sensitivity. The departures from the ideal mesa beam profile are consistent with the mirror imperfections, mainly curvature of the input and folding mirrors and manufacturing imperfections of the MH mirror. These imperfections are much smaller in the high-quality optics used in GWID's, and in particular the MH mirror profile is much easier to produce in the large optics used in astrophysically sensitive interferometers than in the much smaller optics we used.

We have also showed that the sensitivity of the fundamental mesa beam mode profile to mirror tilt is in qualitative agreement with numerical predictions using an FFT model, even given mirror imperfections. In particular, the profile shows marked distortion with only 3-4 μrad tilt angle. This is a first step towards more useful experiments in the future to test autoalignment control of mesa beam cavities. Experiments in the future will also need to study the use of mesa beams in power- and signal-recycled optical cavities.

Acknowledgments

LIGO was constructed by the California Institute of Technology and Massachusetts Institute of Technology with funding from the National Science Foundation and operates under cooperative agreement PHY-0107417. This paper has LIGO Document Number LIGO-P050025-00-D.

The authors also thank GariLynn Billingsley for mirror metrology, Ben Abbott and Paul Russell for electronics and Chiara Vanni for machining pieces of apparatus. We acknowledge the European Gravitational Observatory (EGO) for financial support.

References

1. P. Fritschel, “Advanced LIGO Systems Design”, LIGO T-010075-00-D, available at www.ligo.caltech.edu.
2. E. D’Ambrosio et al., “Reducing Thermoelastic Noise in Gravitational-Wave Interferometers by Flattening the Light Beams”, gr-qc/0409075 v1, 2004.
3. R. O’Shaughnessy, S. Strigin and S. Vyatchanin, “The implications of Mexican-hat mirrors: calculations of thermoelastic noise and interferometer sensitivity to perturbation for the Mexican-hat-mirror proposal for advanced LIGO”, gr-qc/0409050 v1, 2004.
4. E. D’Ambrosio, “Non-spherical mirrors to reduce thermoelastic noise in advanced gravity wave interferometers”, *Phys. Rev. D*, vol.67, ID 102004, 2003.
5. E. D’Ambrosio et al., “Advanced LIGO: non-Gaussian beams”, *Class. Quantum Grav.*, vol. 21, pp. S867-S873, 2004.
6. E. D’Ambrosio, R. O’Shaughnessy, S. Strigin, K. Thorne, and S. Vyatchanin, Status Report on Mexican-Hat Flat-Topped Beams for Advanced LIGO, LIGO-T030009-00; available at <http://docuser.v.ligo.caltech.edu/>
7. J. Agresti and R. DeSalvo, Flat Beam Profile to Depress Thermal Noise, 2005 Aspen Winter Conference, LIGO-G050041-00-Z, available at <http://docuser.v.ligo.caltech.edu/>.
8. J-Y. Vinet, *Class. Quantum Grav.*, vol. 22, pp. 1395-1404, 2005.
9. J. Agresti et al., “Design and Construction of a prototype of a Flat Top beam interferometer and initial tests”, *J. Phys.: Conf. Ser.*, vol.32, pp.301-308, 2006.
10. P. Beyersdorf et al., *Applied Optics*, vol. 45, pp. 6723-6728, 2006.
11. S. Avino. et al., “Generation of non-Gaussian flat laser beams”, *Phys. Lett. A*, vol. 355, pp. 258261, 2006.
12. G.Cella et al., “Seismic attenuation performance of the first prototype of a geometric anti-spring filter”, *Nucl. Instr. and Meth. A*, vol.487, pp.652-660, 2002.
13. M. G. Tarallo, “Experimental study of a non gaussian optical resonator to reduce mirror thermal noise for graviatational waves detectors”, tesi Laurea Specialistica, Univ. Pisa,

LIGO-P050032-00-R, available on LIGO DCC web page.

14. M. Born, E. Wolf , “Principles of optics - 7th ed.”, Cambridge Univ. Press, 1999.

Table 1. Frequency spacing between eigenmodes for the 7.32m long MH cavity prototype. The frequency values are expressed in MHz. The error is 0.3 MHz (sampling spacing).

Peak	Δf_{exp} (MHz)	TEM _{pl} (expected)	$\Delta f(TEM_{pl})$
1	0	00	0
2	0.3783 ± 0.1	01	0.4141
3	1.009 ± 0.1	02	1.0945
4	1.387 ± 0.1	10	1.6542
5	2.018 ± 0.1	03	1.9905
6	2.900 ± 0.1	11	2.8789
7	4.161 ± 0.1	12	4.1754
8	4.414 ± 0.1	20	4.4050
9	5.549 ± 0.1	13	5.5523
10	5.801 ± 0.1	21	6.0031

List of Figure Captions

Fig. 1. Schematic of the mesa beam cavity prototype experimental setup: the two optical benches, the cavity tank, the control electronics and the profile acquisition. Solid lines denote optical signals; dotted lines denote electronic signals. (1) Lenses to eliminate astigmatism, (2) Faraday isolator, (3) mode matching lens, (4) flat input mirror, (5) MH mirror, (6) flat folding mirror, (7, 10) beam imaging lenses, (8) beam dump, (9) wedged attenuating pickoff mirror. Unlabeled items are beam-steering mirrors.

Fig. 2. Schematic view of the mechanical structure showing 3 of the 5 triangular spacers. (i) Flat input mirror, (ii) MH mirror, (iii) thermal shield (dotted line), (iv) vacuum tank (solid line), (v) spacer plate, (vi) Invar rod, (vii) flat folding mirror.

Fig. 3. Surface profiles of the MH test mirror. The transverse pixel dimensions are 0.035 cm.
(a) MH test mirror: global view.
(b) Zoom of the central bump: the pixel colors show the asymmetry of the test mirror. FFT simulations showed a tilt effect of about $0.9 \mu\text{rad}$.

Fig. 4 Misaligned modes.

Fig. 5 Alignment of the fundamental mesa beam with astigmatic flat cavity mirrors: (a) stable, asymmetric single peak, (b) highly sensitive double peak distribution.

Fig. 6 Three-dimensional profile of the mesa fundamental mode.

Fig. 7. One-dimensional profiles of fits to the mesa beam profiles. The top row shows normalized experimental data as measured at the CCD camera. The dashed line is the best fit mesa profile. The bottom row shows profiles extracted from the FFT simulation with best corrective tilt applied. In this case, the transverse scale is taken at the MH mirror.

Fig. 8. High order mesa beam transverse modes: (a) TEM_{10} , (b) TEM_{11} , (c) TEM_{20} .

Fig. 9. The mesa TEM_{10} profile (thick black line). The light gray line show the theoretical mesa TEM_{10} , which better fits the data than a Laguerre-Gauss TEM_{10} mode (dashed line).

Fig. 10. The apparatus used to measure the tilt sensitivity of the mesa beam cavity: (i) Mephisto laser, (ii) HeNe chopper monitor laser, (iii) mode profiler CCD camera, (iv) chopper wheel, (v) He-Ne optical lever laser, (vi) chopper monitor photodiode, (vii) optical

lever quadrant photodiode, (viii) mirror dithering PZT, (ix) function generator.

Fig. 11. Comparison of FFT simulated (thick) and experimental profiles (thin) with same integrated power for various tilts.

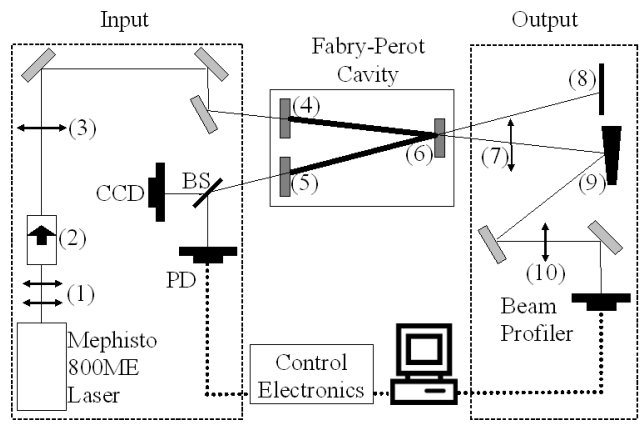


Fig. 1.

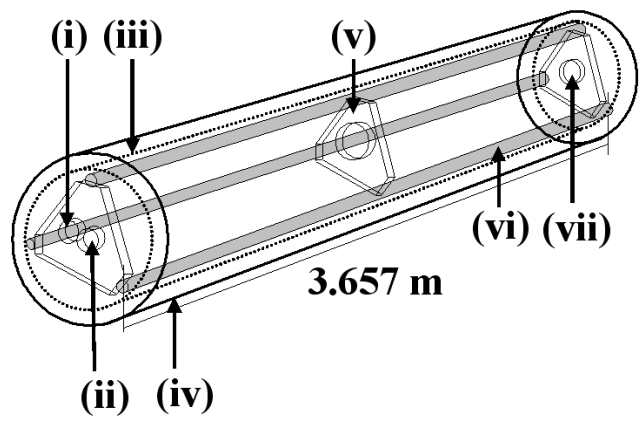
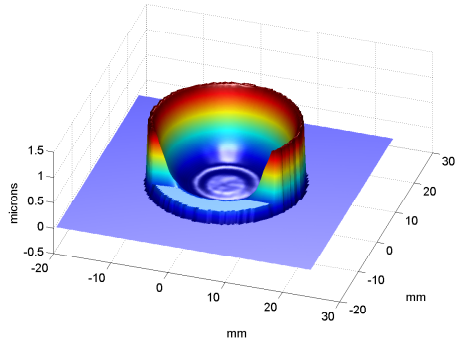
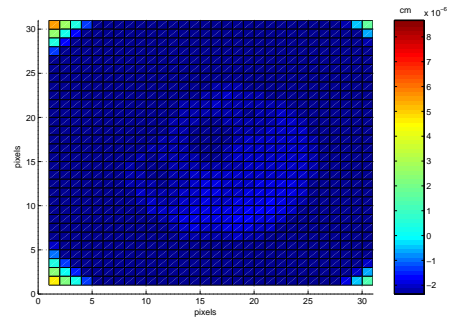


Fig. 2.



(a)



(b)

Fig. 3.

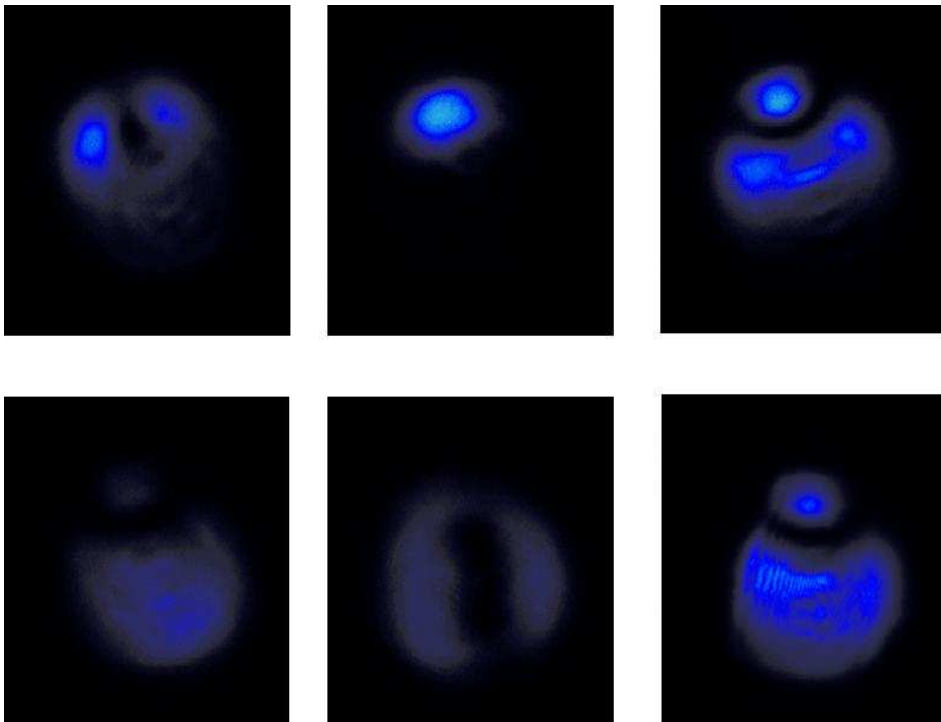


Fig. 4.

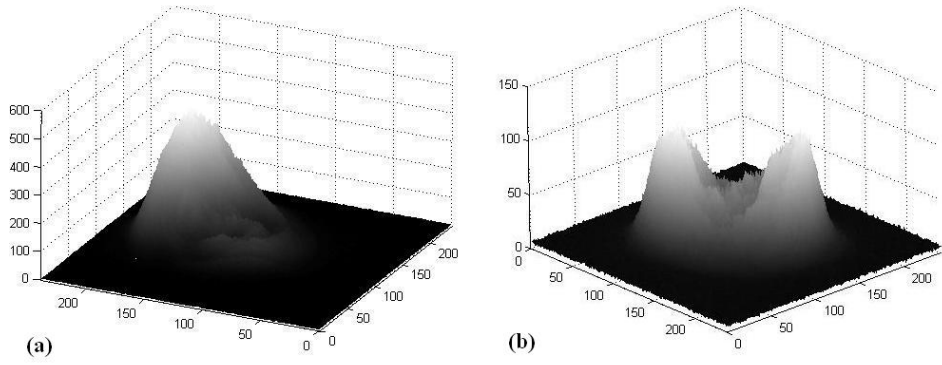


Fig. 5.

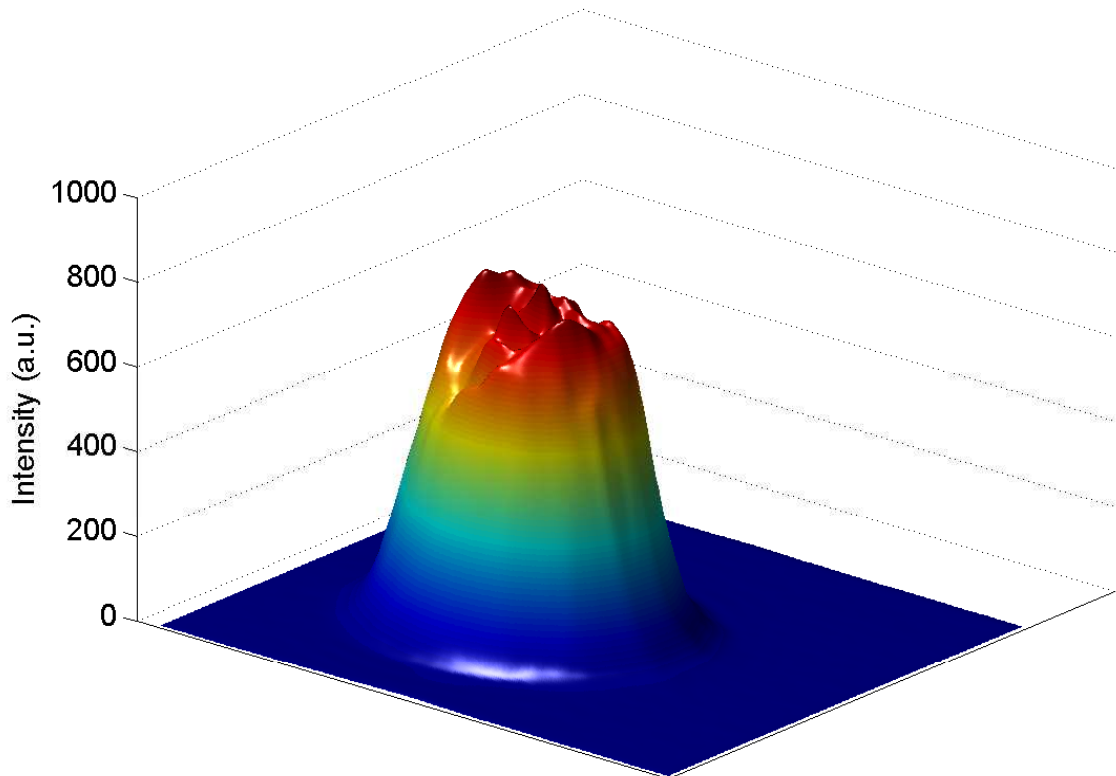


Fig. 6.

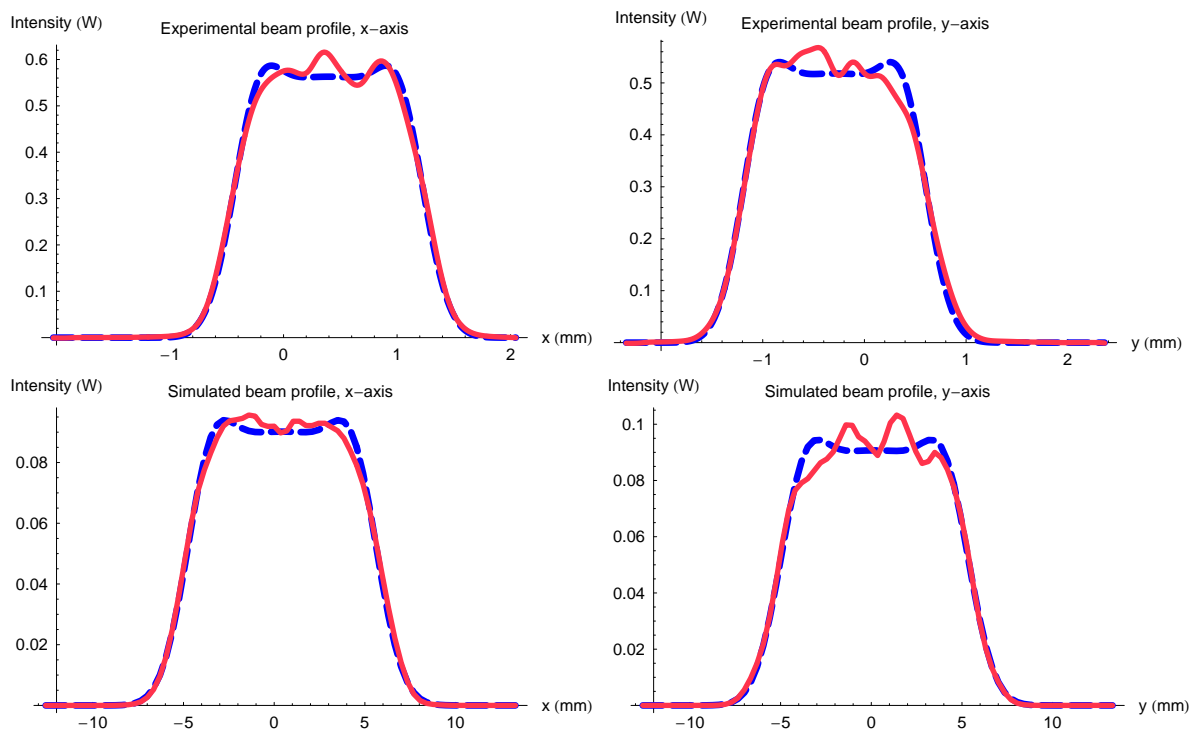
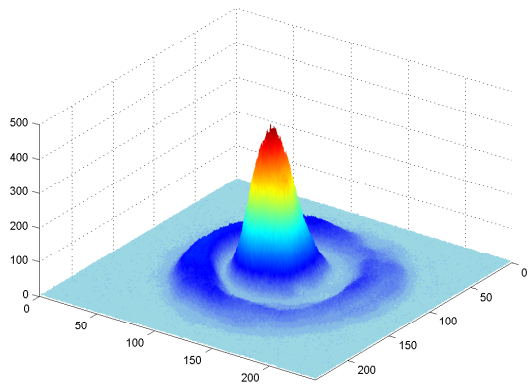
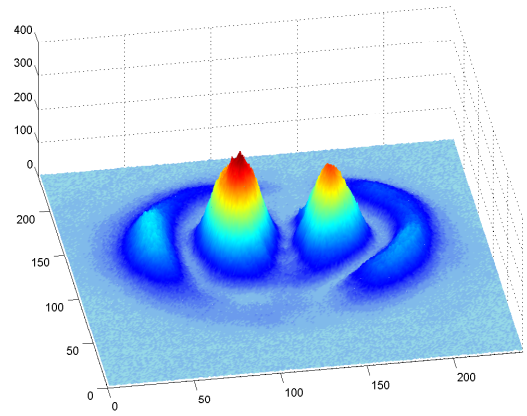


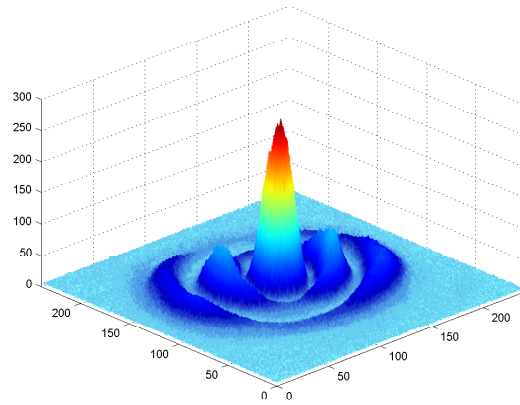
Fig. 7.



(a)



(b)



(c)

Fig. 8.

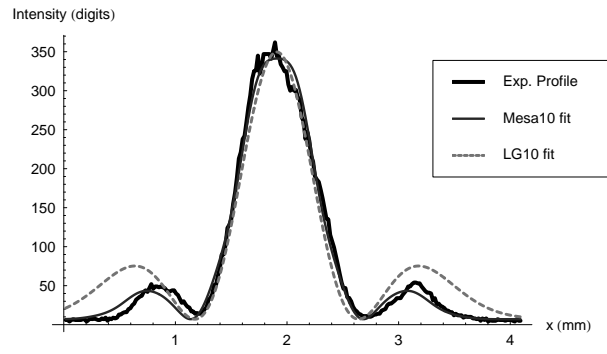


Fig. 9.

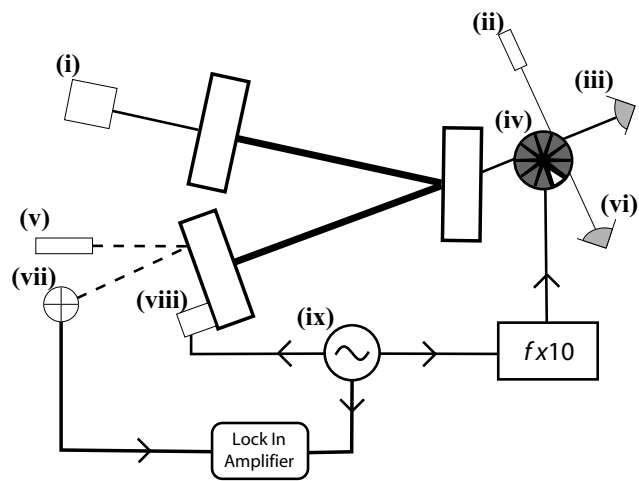


Fig. 10.

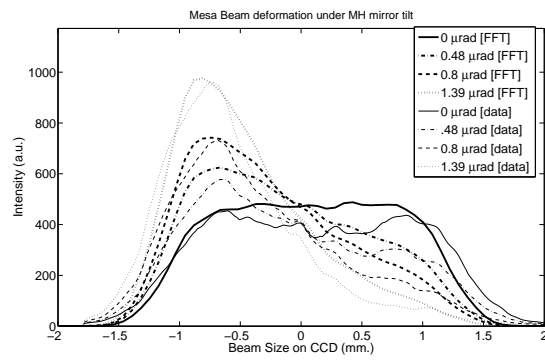


Fig. 11.